STM JOURNALS

International Journal of
Electro-Mechanics and
Material Behaviour

Volume 4, Issue 1, 2026
January–June
DOI Journal: 10.37591/IJEMB

https://journals.stmjournals.com/ijemb

Research IJEMB

Synthesis of a Supercapacitor Based on Nanomaterials

Rone*

Abstract

Demand for various energy storage technologies in electronic and electrical devices continuously goes on increasing. In that context, the objective of this research work is to develop and test an electrode of an energy storage module (supercapacitor) using nickel hydroxide and carbon-based nanocomposite materials. The electrochemical performance of the electrode is enhanced by optimizing synthesis parameters and designing the electrochemical cell. Conventional and all-solid-state supercapacitors are developed with notable electrochemical performance. Pure $Ni(OH)_2$ is deposited on 3D networked nickel foam by the chemical bath deposition process under thermal treatment to develop the electrode. The nanoflower-like structure formed by connecting nanosheets exhibits a porous structure, which leads to faster ion diffusion and shortens the diffusion path of the electrolyte. Electrochemical characterization has been carried out using cyclic voltammetry and galvanostatic charge-discharge. The specific capacitance of 1065 F g^{-1} was observed for the $Ni(OH)_2$/Ni electrode at a current density of 1 A g^{-1}. The electrochemical characterization result demonstrates that the obtained specific capacitance for nanoflower-like $Ni(OH)_2$ was far less than the theoretical specific capacitance of $Ni(OH)_2$, and this is due to the semiconductor nature of nickel hydroxide (poor electrical conductivity ~10^{-17} S cm^{-1}). To improve electrical conductivity, reduced graphene oxide (rGO) having good electrical conductivity and high surface area (2630 m^2g^{-1}) was added to pure $Ni(OH)_2$ to form a nanocomposite of $Ni(OH)_2$/rGO/Ni. The maximum specific capacitance of 1947 F g^{-1} was obtained for the $Ni(OH)_2$/rGO/Ni electrode at a current density of 1 A g^{-1}. Further, to enhance another important parameter, stability, cobalt is doped into $Ni(OH)_2$/rGO/Ni. Addition of cobalt increases electrochemical activity by offering rich redox reactions from both nickel and cobalt, and it reduces electrode resistance and increases oxygen overpotential.

Keywords: Energy storage, nanocomposites, material synthesis, electrode, electrochemical, supercapacitors

INTRODUCTION

Industrial and economic development massively relies on the availability of fossil fuel resources. The energy demand for fossil fuels worldwide was 13.731 billion tons of oil equivalents (BTOE) as of 2012, and it is expected to increase to 18.30 BTOE by 2035 [1, 2].

***Author for Correspondence**
Rone
E-mail: roniesomadder@gmail.com

Assistant professor Department of Mechanical Engineering, Echelon Institute of Technology, Faridabad, Haryana, India

Received Date: February 01, 2026
Accepted Date: February 27, 2026
Published Date: March 10, 2026

Citation: Rone. Synthesis of A Supercapacitor Based on Nanomaterials. International Journal of Electro-Mechanics and Material Behaviour. 2026; 4(1): 23–36p.

However, the depletion of natural resources and uneven distribution cause problems such as economic imbalance, which impacts energy generation and storage, industrial operations, and transportation sectors. In addition, the consumption of fossil fuels generates pollutants such as CO, CO_2, and NO_x, etc., which cause significant environmental damage, such as the greenhouse effect [3]. In this context, many researchers are looking for alternatives to fossil fuel resources. As part of this, the development of renewable energy

sources such as solar, wind, tidal, and geothermal energy has been pursued extensively [4–7].

Apart from biofuels, major renewable sources generate energy in terms of electricity, and advanced storage technology is required to store such generated energy. Hence, there has been a great demand for reliable electrochemical energy storage devices with excellent electrochemical performance, such as batteries, fuel cells, and supercapacitors [8]. Among them, supercapacitors have attracted more attention owing to their characteristics, such as fast storage capability, flexible packaging, wide temperature range (-40°C to 70°C), high-security coefficient (long-time use with little maintenance), improved cyclic stability, and superior lifespan (>1000000) [9]. The performance comparison for battery, supercapacitor, and conventional capacitors is given in Table 1, which indicates supercapacitor facing major issues regarding poor energy density as compared to battery technology. However, recent advancements in electrode materials and electrolytes have solved the issue of poor energy density [10]. Because of this, year by year research work on supercapacitors goes on increasing, as indicated by the number of publications accessed on Google Scholar on this topic shown in Figure 1. This also indicates how property enrichment has been performed in electrode materials [11].

The supercapacitor, also known as an ultracapacitor, was first developed in 1957 by General Electric during experimentation on porous carbon. General Electric engineers found that porous carbon can store charge by forming a double layer. The same double-layer effect was rediscovered by researchers at Ohio University in 1966 when they were working on fuel cell design. In this design, two activated charcoal electrodes separated by a thin, porous insulator were used, and the same mechanical design is used to date for electric double-layer capacitors [12]. The first commercialized supercapacitor was developed by Sohio. Between 1975 and 1981, Conway proposed a new type of supercapacitor where a RuO_2 film was used in aqueous H_2SO_4, which demonstrated charge storage based on surface redox reactions [13]. The Nippon Electric Company (NEC) in 1978 first referred to the term “Supercapacitor” in 1978 and used it in practical application as backup power for computer memory [4, 14–18].

The supercapacitor is an energy storage device having very high-power density and low internal resistance; these properties make it able to store and deliver energy at higher rates than the battery. A supercapacitor consists of two electrodes separated by a dielectric film in an electrolyte. The electrode and electrolyte materials are the most important parameters for the electrochemical performance of supercapacitors [8].

Fundamentals of Supercapacitor

Various parameters play an important role in determining the final performance of supercapacitors. In this section, all such parameters affecting electrochemical performance are discussed.

Types of Supercapacitors

Based on the energy storage mechanism, supercapacitors are grouped into three categories: electrochemical double-layer capacitors, pseudocapacitors, and hybrid capacitors (Figure 2).

Table 1. Comparison between supercapacitor and battery based on properties [10].

Parameters	Electrochemical capacitor	Battery
Energy density	Low	High
Power density	High (1–10 kW kg^{-1})	Low (150 W kg^{-1})
Charge-discharge cycle	10^5–10^6	500–10^4
Self-discharge time at room temperature	Days–week	Months
Lifetime at room temperature (years)	5–10	3–5
Cell voltage (Volts)	1.2–3.8	2.5–4.2

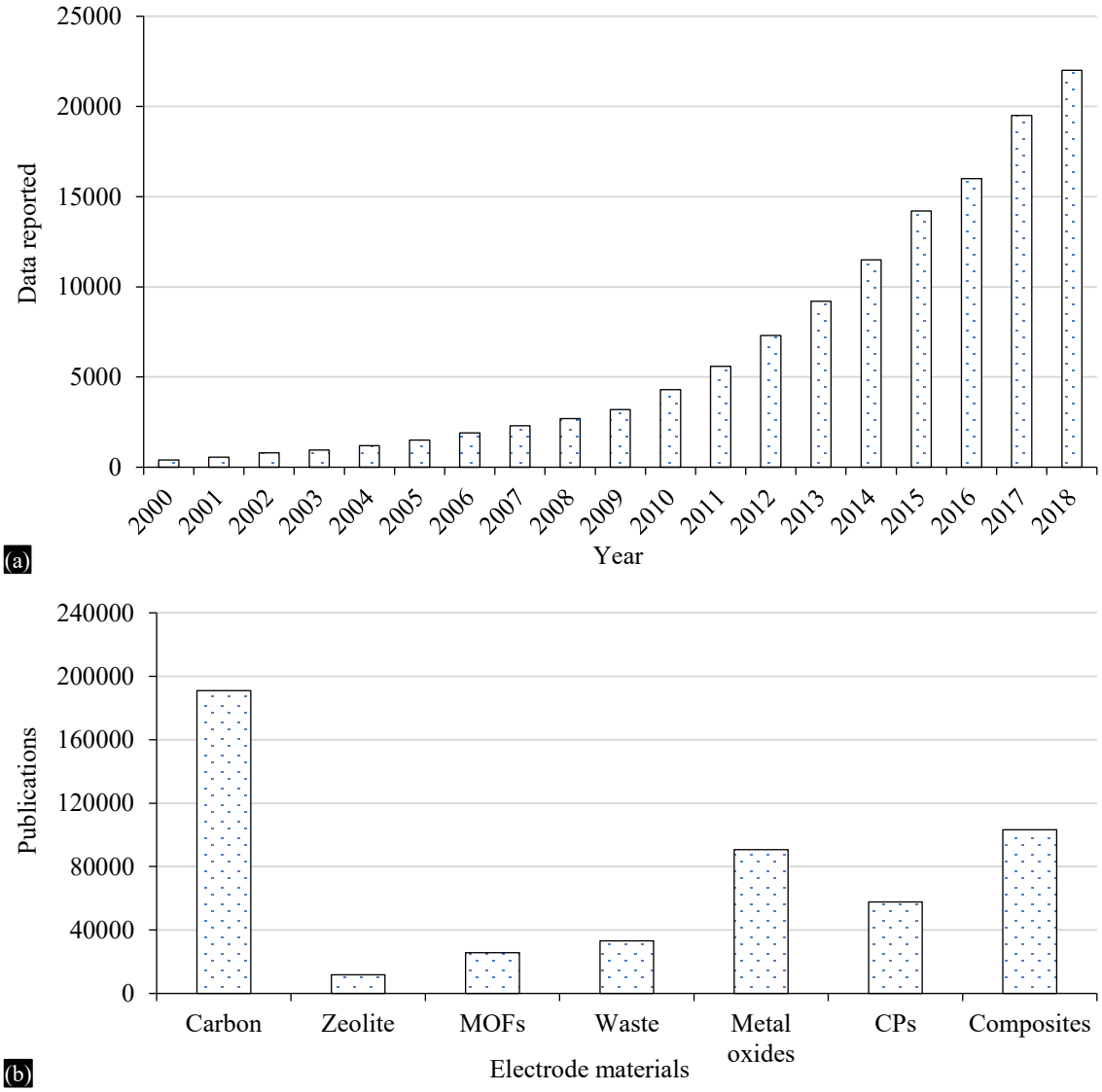

Figure 1. Statistical survey of research activities on supercapacitors. (a) Number of publications (including journal articles, books, and other scholarly literature) related to supercapacitors from 2000–2018, obtained using "supercapacitor" as the search keyword. (b) Distribution of publications based on different electrode materials used in supercapacitor research, including carbon, zeolite, metal–organic frameworks (MOFs), waste-derived materials, metal oxides, conducting polymers (CPs), and composites.

Electrochemical Double-Layer Capacitor

In an electrochemical double-layer capacitor (EDLC), the charge storage mechanism is based on nanoscale charge separation at the electrochemical interface between the electrolyte and electrode. The charge storage mechanism is completely non-Faradaic, and no oxidation-reduction reaction occurs. Owing to the absence of charge transfer betweenelectrodes, EDLC have a superior life cycle [19–25]. Materials with high surface areas, such as activated carbon, graphene, and carbon aerogel (carbon-based materials), exhibit EDLC-type behavior. EDLCs are constructed using two carbon-based electrodes, an electrolyte, and a separator. When voltage is applied, there is an accumulation of charge on the electrode surface; due to the potential difference, oppositely charged electrolyte ions are attracted towards respective electrodes and form a double layer (Figure 3). To avoid recombination, a double layer is formed, and this double layer increases with increasing specific surface area and decreases with distance between two electrodes [4].

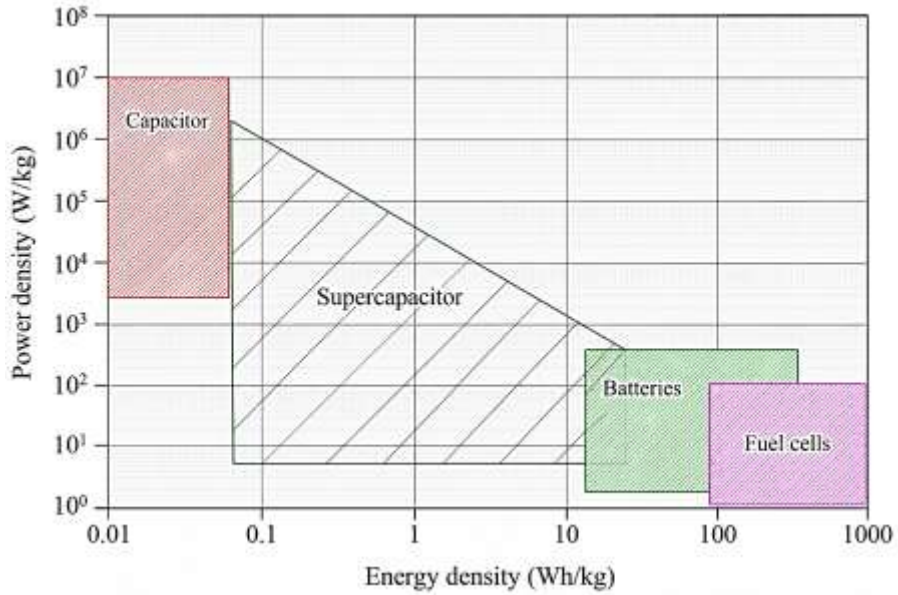

Figure 2. Ragone plot for various electrical energy storage devices (specific power against specific energy).

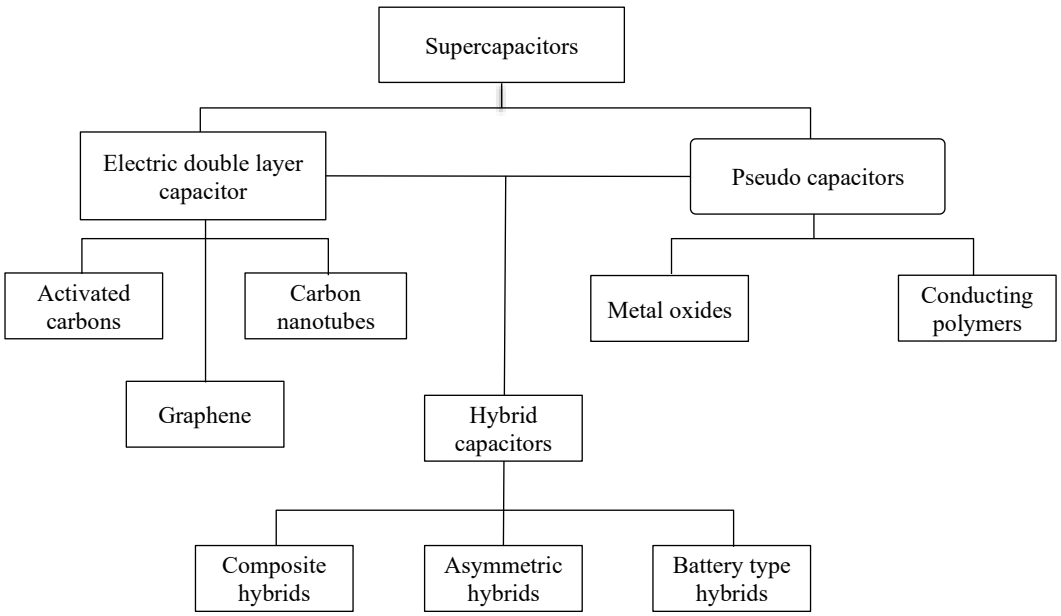

Figure 3. Taxonomy of supercapacitor

The charge storage mechanism of the EDLC allows fast energy uptake and delivery, leading to superior power performance. In addition, because of the absence of chemical reactions, swelling, which is generally observed in battery electrodes, is avoided. The electrostatic surface charge mechanism limits the energy density of the EDLC; hence, more research has focused on enhancing the energy density and operating temperature range of the EDLC electrodes [6].

Pseudocapacitor

In the case of pseudocapacitors, charges are stored through a faradaic process, where charges are transferred across the electrodes. When potential applied to pseudocapacitor redox reaction (oxidation-reduction) occurs at the electrodes, where charges pass across the double layer, and faradaic current passes through the cell. Due to the reversible faradaic process, supercapacitors allow a higher specific capacitance and energy density than EDLC. Transition metal oxides and conducting polymers exhibit

pseudocapacitive behavior. Even though pseudocapacitor materials have a superior energy density, they suffer from poor stability and lower power density because the reversible faradaic reaction generates swelling of the electrode [16, 17].

Hybrid Capacitor

Hybrid capacitors have been developed to combine the advantages of EDLCs and pseudocapacitors. EDLCs possess excellent stability and superior power density, whereas pseudocapacitors possess higher energy density. A hybrid capacitor exhibits all these characteristics. A hybrid capacitor combines energy source from a battery-like electrode and a power source from a capacitor-like electrode. By using an appropriate combination of these two electrodes, it is possible to achieve a high-performance hybrid system. Several combinations have been tested till now as positive and negative electrodes in various types of electrolytes such as aqueous, inorganic, and ionic [18]. Currently, major research has focused on three types of systems:

1. *Composite:* Composite electrodes combine EDLC materials with pseudocapacitive materials in a single electrode, such as RuO_2/graphene. Both physical and chemical storage mechanisms are involved in a single electrode [26–30]. Carbon-based materials offer a double-layer charge and high specific area, which enhances the contact between the pseudocapacitive material and electrolyte, while reversible faradaic reactions enhance the capacitance of the composite material. Currently, binary and ternary composite electrodes are used in supercapacitors.
2. *Asymmetric:* The asymmetric supercapacitor couples an EDLC-type electrode with a pseudocapacitive-type electrode in a single cell. This system combines a faradaic process with a non-faradaic reaction, where a carbon-based material is coupled with a metal oxide or conducting polymer.
3. *Battery-type:* In a battery-type hybrid system, two different types of electrodes are combined to form a cell. A supercapacitor-type electrode was combined with a battery-type electrode. In this way, both battery and supercapacitor properties can be utilized (Figure 4).

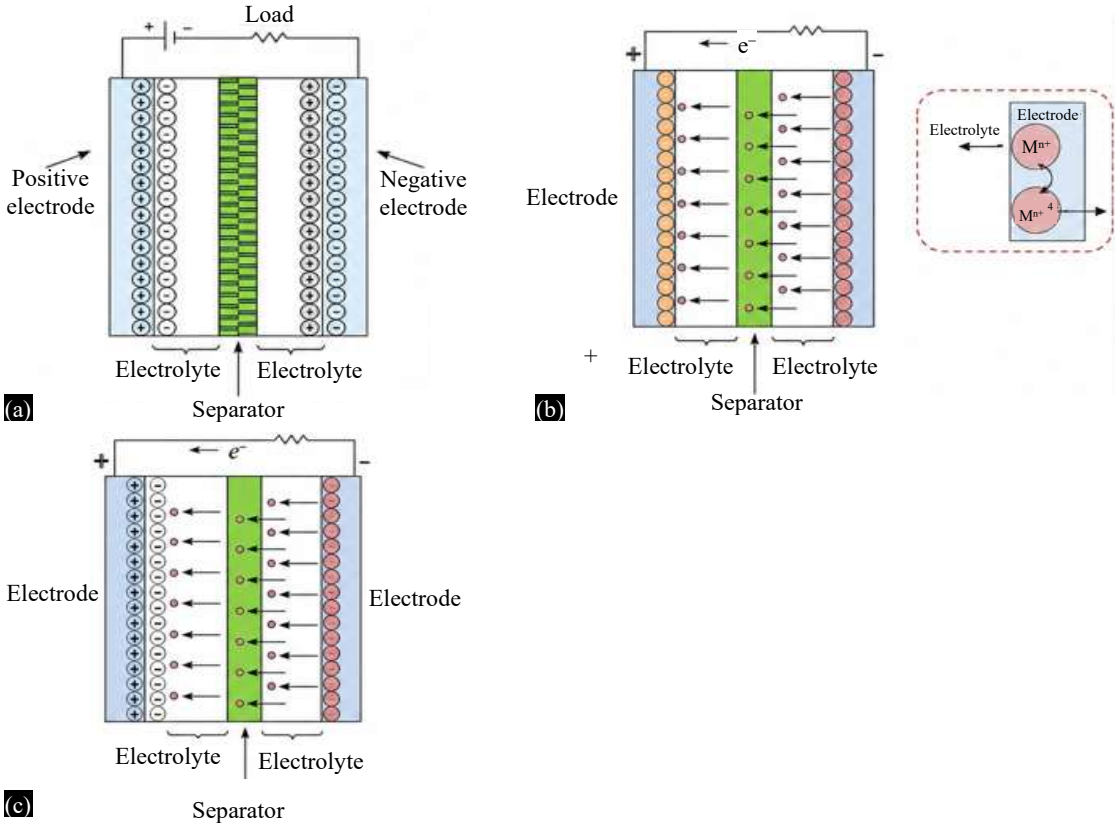

Figure 4. Schematic representation of supercapacitor types: (a) EDLC-type; (b) pseudocapacitor type; (c) hybrid capacitor-type (the figure is not to scale) [18].

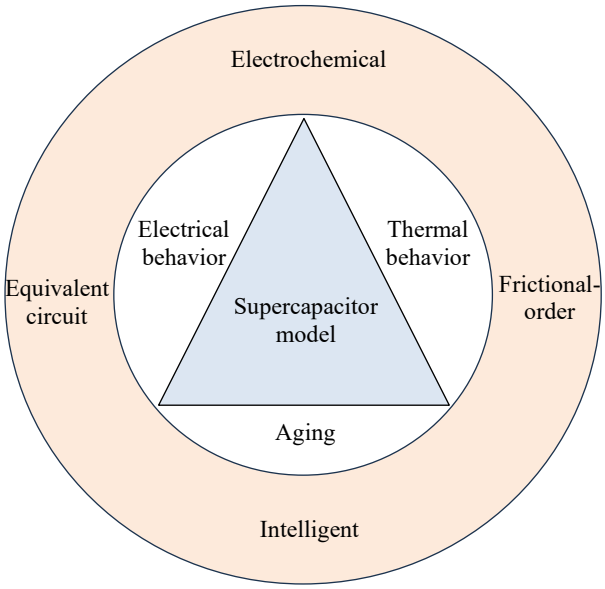

Figure 5. Various models are available for Supercapacitor modeling.

ELECTROCHEMICAL MODELING

Mathematical modeling and numerical solutions play a vital role in the design and performance estimation of advanced energy storage systems, such as batteries and supercapacitors. However, there are challenges in deriving and solving this model analytically and numerically, such as a model that intends to cover all physical and chemical factors that must be considered, conversion of charge, species, and energy along with appropriate relationships for double-layer charging and redox reactions. In addition, it should apply to all functional layers and groups within the cell at differentscales, such as the macroscale or microscale [12]. The characteristics obtained in the process are closely related to the parameters used in the process and mainly depend on the physical, chemical, electrochemical, electrical, and crystallographic parameters of the electrode and electrolyte materials, as well as the design parameters of its components and the supercapacitor as a whole (Figure 5).

Hence, for modeling supercapacitors and predicting their performance, such as energy and capacitance, proper knowledge of their component parameters is necessary [13].

Artificial Neural Network

The mathematical model and electrical model obtained the best performance report, but sometimes it becomes very cumbersome; for example, in the case of mathematical modeling, non-linear equation formulation becomes very difficult. In this case, an artificial neural network (ANN) can be used for any linear or non-linear system [13]. ANN can be applied in a wide variety of scientific and engineering applications, such as control, modeling, and identification [14]. Recently, ANNs have been used to predict the performance of supercapacitors and batteries [15]. The structural unit of ANN is identical to that of biological neurons, where inputs are weighted, summed, and transformed as output. A set of processing elements in ANN is called a neuron (Figure 6). Every neuron corresponds to a function from one or more inputs to a single output. The principle behind ANN is that, instead of programming, they learn to make predictions.

An ANN is composed of three elements: the input layer, hidden layer, and output layer [15]. The information transmitted to the node (neurons) in the hidden layer is amplified by weight W_{ij}, and the piece of information coming to each node is summed, transformed, and redistributed to further hidden nodes or the output layer. The schematic diagram of an ANN is shown in Figure 6. Let S = (S_1, S_2, S_3…S_n) represent the n inputs applied to the system [31–36].

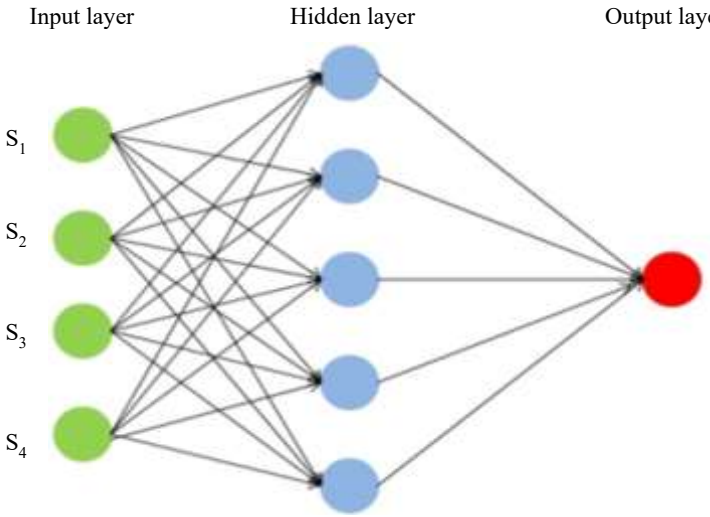

Figure 6. Artificial neural network with a single hidden layer.

Table 2. Artificial neural network parameters and architecture.

ANN parameters	Number/type
Number of neurons at input	2
Number of neurons at output	1
Number of neurons at hidden layer	10
Activation function	Sigmoid function
Learning rule	Levenberg–Marquardt backpropagation algorithm

Parameter Selection

The present model focuses on the modeling of cyclic voltammetry (CV) behavior to predict specific capacitance. The multilayer perception concept is the basis for the present ANN model. The scripting was performed using MATLAB 2016 R1. Various learning algorithms are used in the training network; this work is trained using the Levenberg–Marquardt backpropagation (BP) algorithm. The model of three layers of feed-forward ANN consists of an input layer, hidden layer, and output layer (Table 2). The number of neurons in the hidden layer is decided by the number of input neurons as per the rule of thumb (size of hidden neurons roughly twice the size of input neurons). The sigmoid function is used as an activation or transfer function for further improvement in performance [37–42].

In this modeling, data generated from CV characterization for $Ni(OH)_2$ were used for training and testing the ANN model. The current density was obtained within the potential scan window for the forward oxidation and reverse reduction cycles. The potential scan and cycle were used as input parameters for the ANN, while the obtained current was used as the output. Among the data used, 80% was used for training, while 20% of the data was used for testing. More than 1000 iterations were used to achieve the correct output [43–48].

MODEL ANALYSIS

In this model, two input neurons, potential and redox cycle (oxidation and reduction), approx. ten hidden layers, and one output layer for current density are used, which is shown in Figure 7. The obtained error values were very small, indicating that the ANN can predict the appropriate specific capacitance once the current density is predicted (Table 3). If we know the potential for a specific material, we can predict the current density, which leads to the calculation of the specific capacitance by substituting the value in the model. Such an ANN model can be used to predict the specific capacitance, energy density, and power density using various material properties. The data generated from electrochemical characterization can be used for training models, and such prepared models can save the time required for rigorous experimentation.

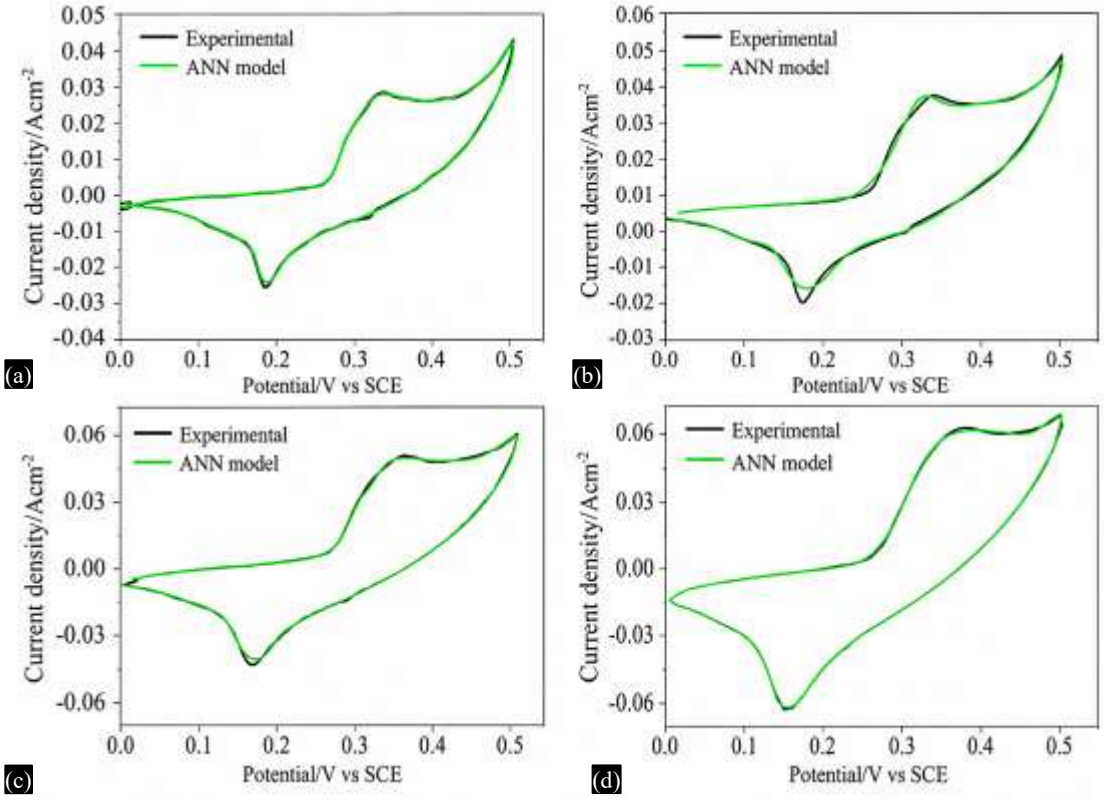

Figure 7. Comparison between cyclic voltammetry (CV) curves obtained from experimentation and ANN modeling at (a) 10 mV s^{-1}, (b) 20 mV s^{-1}, (c) 30 mV s^{-1}, (d) 40 mV s^{-1} obtained from a three-electrode workstation.

Table 3. Comparison of results obtained from the ANN model and Experiments.

Scan rate (mVs^{-1})	Experimental capacitance (Fg^{-1})	ANN predicted capacitance (Fg^{-1})	Error in %
10	958	954	0.41
20	656	652.3	0.56
30	645	641.4	0.55
40	639	636.2	0.43

DEVELOPMENT OF ENERGY STORAGE MODULE

Negative Electrode Preparation

Selection of Material

Asymmetric supercapacitors composed of one battery-type faradaic electrode (higher energy density) and one capacitor-type electrode (higher power density) can exhibit superior energy density, power density, and cycle life [14]. An asymmetric supercapacitor can fully utilize the differential potential window of the electrode materials, thereby providing a maximum potential window for the cell. Hence, the selection of proper materials for a negative electrode as per the positive electrode used to assemble a high-performance asymmetric supercapacitor is critical [14, 15].

In this study, Fe_2O_3 deposited on nickel was selected as the negative electrode. Among the metal oxides used as negative electrodes, Fe_2O_3 has attracted attention due to its characteristics such as high theoretical capacitance, ideal potential window, low cost, and environmental friendliness [38, 47]. The CV curve is shown in Figure 8, and the potential window obtained for Fe_2O_3 was -0.85 to 0.0 V [39]. For the synthesized positive electrode Ni.Co layered double hydroxide (LDH)/reduced graphene oxide (rGO) exhibited a potential window of 0.0 V to 0.5 V; hence, after assembling these two electrodes as an asymmetric supercapacitor, the overall cell voltage can cross the 2.5 V limit.

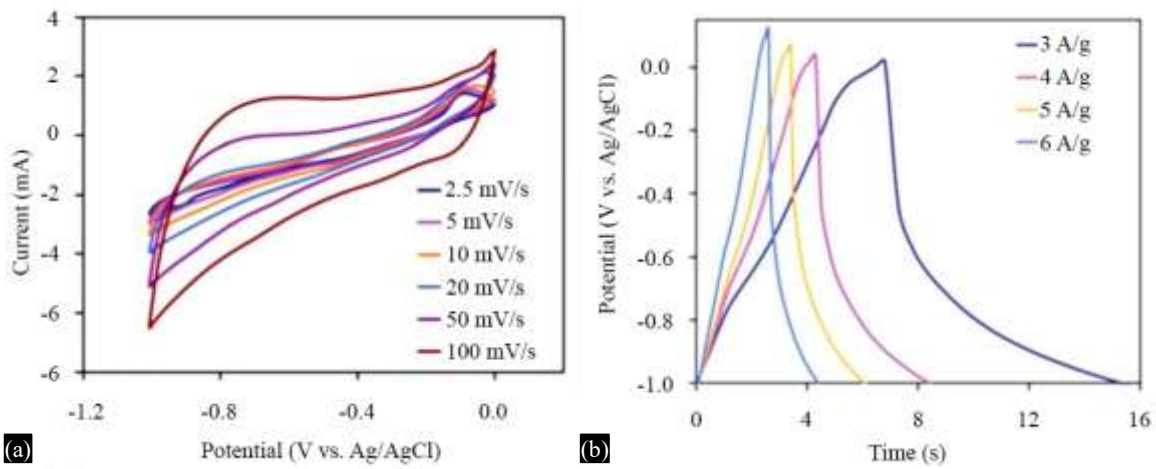

Figure 8. Cyclic voltammetry of Fe_2O_3 at scan rates (a) 2.5, 5, 10, 20, 50, 100 mV s^{-1}, (b) galvanostatic charge-discharge (GCD).

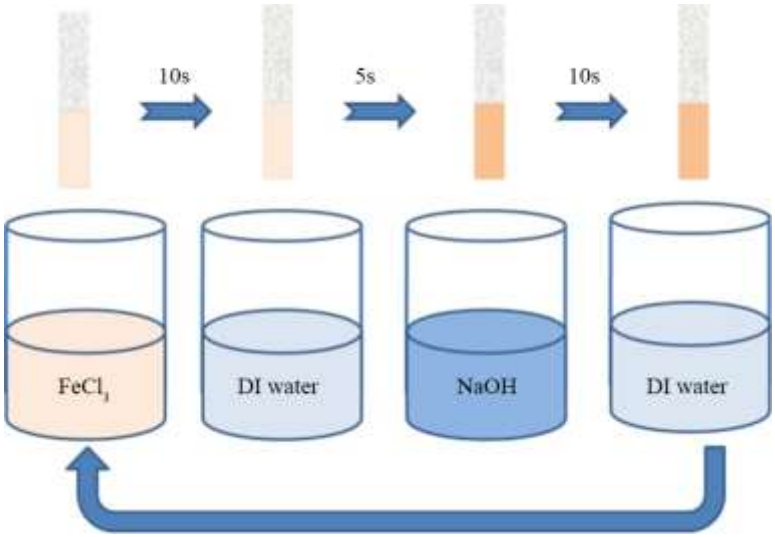

Figure 9. Schematic process of successive ionic layered adsorption and reaction (SILAR)

Synthesis Process

Nanostructured Fe_2O_3 was deposited on nickel foam using a simple successive ionic layer adsorption and reaction (SILAR) method with four beakers, as schematically shown in Figure 9. The solutions of 0.01 M $FeCl_3$ and 1 M NaOH were used as cationic and anionic precursors, respectively. The piece of nickel foam (3 cm × 2 cm) was cleaned with diluted HCl solution to remove oxides and dirt present on the substrate. The cleaned nickel foam was initially dipped in cationic solution for 10 s so Fe^{+3} ions can be adsorbed on the surface of the nickel foam. Next, the substrate was dipped in deionized water (DI) water to remove loosely bound species.

After that, the substrate was dipped into an anionic solution for 10 s, where OH^- ions react with Fe^{+3} to form Fe_2O_3. Finally, the substrate was dipped in DI water for 5s so that loosely bound species were removed. These 150 cycles were repeated to obtain the required layer thickness of Fe_2O_3.

RESULTS FOR ELECTROCHEMICAL PERFORMANCE

The excellent performance of Ni.Co LDH/rGO deposited on nickel foam was used for fabrication of an all-solid-state asymmetric supercapacitor with Fe_2O_3 deposited on Ni foam. In this module, Ni.Co LDH/rGO acts as the positive electrode and Fe_2O_3 as the negative electrode. The PVA/KOH gel was

used as both the electrolyte and separator. The assembled all-solid-state asymmetric supercapacitor was electrochemically tested using cyclic voltammetry (CV) and galvanostatic charge-discharge (GCD) techniques. Figure 10 shows the CV curve for the asymmetric cell Ni.Co LDH/rGO/Ni//Fe_2O_3/Ni at scan rates of 10, 20, 40, 60, 80, and 100 mV s^{-1}.

The overall voltage window obtained for the CV curve was -0.5 to 1.6 V. The CV profile demonstrates the hybridized capacitance obtained from the electrical double-layer capacitance and pseudocapacitance. The overall potential obtained for the assembled asymmetric supercapacitor is 2.1 V, which is higher than the conventional battery (1.5 V) for a single cell. The asymmetric cell developed Ni.Co LDH/rGO/Ni//Fe_2O_3/Ni exhibited a potential window of 2.1 V, while specific capacitance of 90.20 F g^{-1} is calculated from the CV profile at a scan rate of 10 mV s^{-1} (Figure 10(a)). Figure 10(b) shows the GCD profile for the Ni.Co LDH/rGO/Ni//Fe_2O_3/Ni assembled asymmetric supercapacitor at current densities of 1, 2 and 3 A g^{-1}. The non-linear correlation with the potential obtained from the GCD curve suggests pseudocapacitive behavior for the module.

Calculation for single module:

Discharge time $\Delta t = 129$ s

Active mass = 0.566 g (0.5016 + 0.0544) Voltage window = 2.1 V

$Cs = 129 \times 1/(2.1 \times 0.566) = 110.48$ Fg^{-1} $E = 110.20 \times 2.1^2/7.2 = 67.669$ Wh kg^{-1}

$P = E \times 3600/\Delta t = 64.32 \times 3600/129 = 1888.43$ W kg^{-1}

Figure 11(a) shows the variation in specific capacitance with current density for the device fabricated with Ni.Co LDH/rGO with an Fe_2O_3 negative electrode. The specific capacitance decreased slowly with increasing current density, indicating the excellent rate capability of the assembled device. The cyclability of the prepared device was evaluated at 5000 cycles.

Figure 11(b) shows the curve of specific capacitance versus cycles. The curve obtained demonstrated that the specific capacitance increased to approximately 1000 cycles, which may be due to the availability of intrinsic active mass at the nickel foam 3D network. After 1000 cycles, the specific capacitance decreased and stabilized at 2000 cycles and then decreased slowly. The obtained graph shows that the developed cell exhibited excellent energy and power densities and a superior cycle life.

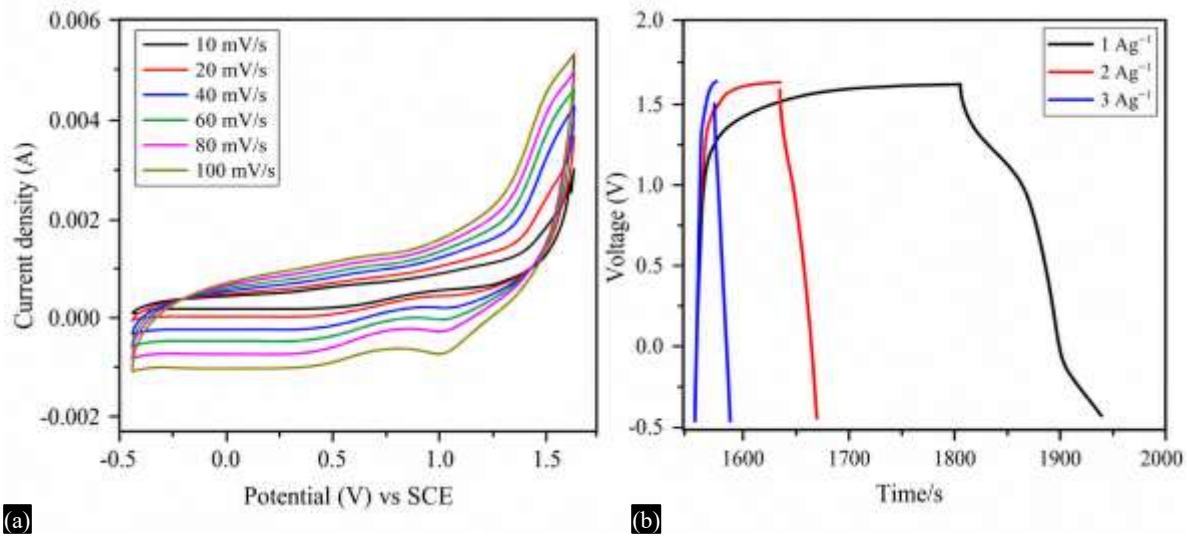

Figure 10. (a) Cyclic voltammetry of Ni.Co LDH/rGO/Ni//Fe_2O_3/Ni at scan rates 10, 20, 40, 60, 80 and 100 mV s^{-1}, (b) galvanostatic charge-discharge of Ni.Co LDH/rGO/Ni//Fe_2O_3/Ni at current densities 1, 2 and 3 A g^{-1}.

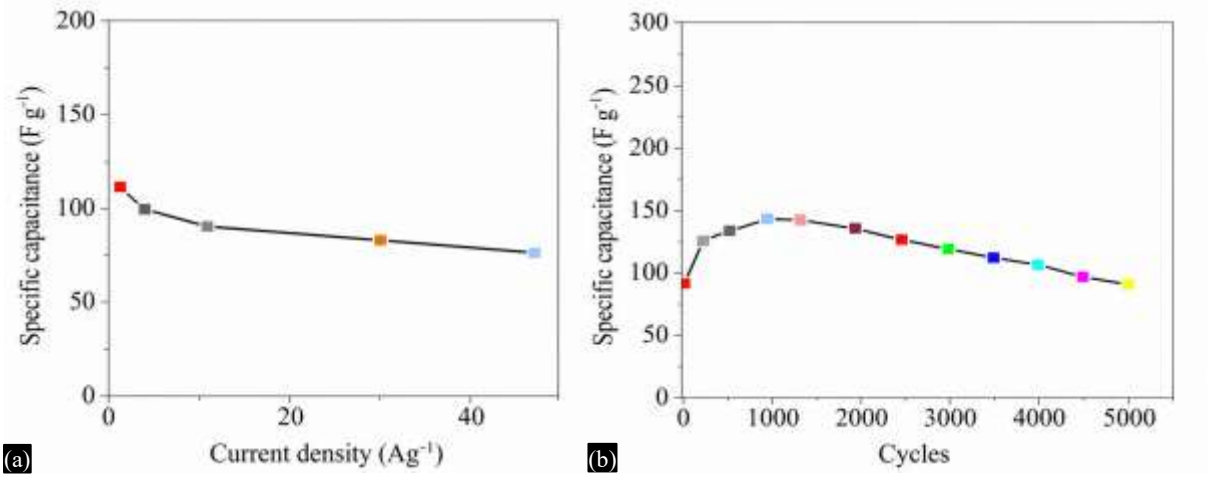

Figure 11. (a) Specific capacitance versus current density. (b) Cycle versus specific capacitance for energy storage module prepared from Ni.Co LDH/rGO/Ni//Fe_2O_3/Ni.

CONCLUSIONS

- Based on the higher theoretical specific capacitance and environmental friendliness, nickel hydroxide $Ni(OH)_2$ materials were selected. The expected electrochemical performance and intrinsic properties of the electrode material were achieved through the chemical bath deposition synthesis process. This process was also found to be useful for fabricating binder-free electrodes by directly depositing materials on the substrate. The electrochemical performance measured for $Ni(OH)_2$ deposited on nickel foam exhibited a specific capacitance of 1065 F g^{-1} at a current density of 1 A g^{-1}.
- Owing to the semiconductor nature of $Ni(OH)_2$, it possesses lower electrical conductivity; hence, to enhance the electrical conductivity of $Ni(OH)_2$, highly conductive reduced graphene oxide (rGO) was combined with nickel hydroxide, which not only improved electrical conductivity but also the specific surface area.
- nanosheet of $Ni(OH)_2$ grown on an rGO sheet uniformly spread on a nickel foam network exhibited higher porosity, which allows easy access to the electrolyte. The specific capacitance obtained for $Ni(OH)_2$/rGO was 1947 F g^{-1}.
- Furthermore, due to the cobalt doping in $Ni(OH)_2$, the stability of the composite improved. The addition of cobalt transformed the nanosheet morphology into nanorods, and Ni.Co LDH nanorods were grown vertically on rGO sheets that were uniformly spread on nickel foam, further increasing the porosity and specific surface area of the electrode. The synthesized sample showed a superior specific capacitance of 2957 F g^{-1}, which is nearly equal to the theoretical specific capacitance of $Ni(OH)_2$ (~3000 F g^{-1}). This nanomaterial was found to be more suitable for electrodes.
- An electrochemical model was developed using an ANN based on the cyclic behavior of the material to predict the specific capacitance of nickel hydroxide Ni $(OH)_2$ based nanomaterials. The specific capacitance measured from the ANN model and in the experiments showed a deviation of within 1%. Thus, the developed model can be used for the prediction of capacitance from available data and will reduce experimental work, time, and cost in further research.
- In order to verify the electrochemical performance of the synthesized electrode Ni.Co LDH/rGO, an all-solid-state asymmetric supercapacitor (energy storage module) was successfully developed with Ni.Co LDH/rGO/Ni as a positive electrode and Fe_2O_3/Ni as a negative electrode. The negative electrode Fe_2O_3/Ni exhibited a differential potential window, which is reflected in the developed cell Ni.Co LDH/rGO/Ni//Fe_2O_3/Ni overall voltage as 2.1 V.
- The PVA/KOH gel was successfully used as both the electrolyte and separator. The specific capacitance for the energy storage module measured from the GCD curve delivered 110.9 F g^{-1} at a current density of 1 Ag^{-1} which is higher than the values obtained in the literature.

Future Scope

- Nanomaterials with three metal oxide combinations can be tested as electrode materials. Apart from nano-flowers and nanorods, other nanostructures with high surface areas and porosities may be obtained by changing the synthesis process parameters or process. An electrochemical ANN model based on parameters such as surface-to-volume ratio, pore size, and scan rate can be developed for prediction of electrochemical performance.
- Asymmetric cells can be developed using ionic or redox electrolytes, allowing the voltage to reach up to 4 V. Negative electrode materials other than Fe_2O_3 may be synthesized to achieve a higher active mass. The design of asymmetric supercapacitors can be modified, such as in the case of sandwich or layer-by-layer designs.

REFERENCES

1. Chu S, Cui Y, Liu N. The path towards sustainable energy. Nat Mater. 2016;16:16–22. doi:10.1038/nmat4834.
2. Singh S, Jain S, Ps V, Tiwari AK, Nouni MR, Pandey JK, et al. Hydrogen: a sustainable fuel for future of the transport sector. Renew Sustain Energy Rev. 2015;51:623–33. doi:10.1016/j.rser.2015.06.040.
3. Dhepe P, Tomishige K, Wu KCW. Catalytic conversion of biomass. ChemCatChem. 2017;9:2613-4. doi:10.1002/cctc.201700884.
4. Trancoso R, Larsen JR, McVicar TR, Phinn SR, McAlpine CA. CO_2-vegetation feedbacks and other climate changes implicated in reducing base flow. Geophys Res Lett. 2017;44:2310-8. doi:10.1002/2017GL072759.
5. Milano J, Ong HC, Masjuki HH, Chong WT, Lam MK, Loh PK, et al. Microalgae biofuels as an alternative to fossil fuel for power generation. Renew Sustain Energy Rev. 2016;58:180-97. doi:10.1016/j.rser.2015.12.150.
6. Weigelt C, Shittu E. Competition, regulatory policy, and firms' resource investments: the case of renewable energy technologies. Acad Manage J. 2016;59:678–704. doi:10.5465/amj.2013.0661.
7. Azcárate C, Mallor F, Mateo P. Tactical and operational management of wind energy systems with storage using a probabilistic forecast of the energy resource. Renew Energy. 2017;102:445-56. doi:10.1016/j.renene.2016.10.064.
8. Iro ZS, Subramani C, Dash SS. A brief review on electrode materials for supercapacitor. Int J Electrochem Sci. 2016;11:10628-43. doi:10.20964/2016.12.50.
9. Rakhi RB, Chen W, Cha D, Alshareef HN. High performance supercapacitors using metal oxide anchored graphene nanosheet electrodes. J Mater Chem. 2011;21:16197. doi:10.1039/C1JM12963E.
10. Wang G, Zhang L, Zhang J. A review of electrode materials for electrochemical supercapacitors. Chem Soc Rev. 2012;41:797–828. doi:10.1039/C1CS15060J.
11. Raza W, Ali F, Raza N, Luo Y, Kim KH, Yang J, et al. Recent advancements in supercapacitor technology. Nano Energy. 2018;52:441-73. doi:10.1016/j.nanoen.2018.08.013.
12. Kate RS, Khalate SA, Deokate RJ. Overview of nanostructured metal oxides and pure nickel oxide (NiO) electrodes for supercapacitors: a review. J Alloys Compd. 2018;734:89–111. doi:10.1016/j.jallcom.2017.10.262.
13. Dubal DP, Chodankar NR, Kim DH, Gomez-Romero P. Towards flexible solid-state supercapacitors for smart and wearable electronics. Chem Soc Rev. 2018;47:2065–2129. doi:10.1039/C7CS00505A.
14. Dubal DP, Gomez-Romero P, Sankapal BR, Holze R. Nickel cobaltite as an emerging material for supercapacitors: an overview. Nano Energy. 2015;11:377-99. doi:10.1016/j.nanoen.2014.11.013.
15. Wang Y, Song Y, Xia Y. Electrochemical capacitors: mechanism, materials, systems, characterization and applications. Chem Soc Rev. 2016;45:5925-50. doi:10.1039/C5CS00580A.
16. Lu Q, Chen JG, Xiao JQ. Nanostructured electrodes for high-performance pseudocapacitors. Angew Chem Int Ed Engl. 2013;52:1882-9. doi:10.1002/anie.201203201.

17. Yang S, Bachman RE, Feng X, Müllen K. Use of organic precursors and graphenes in the controlled synthesis of carbon-containing nanomaterials for energy storage and conversion. Acc Chem Res. 2013;46:116-28. doi:10.1021/ar3001475.
18. Wu HB, Zhang G, Yu L, Lou XWD. One-dimensional metal oxide-carbon hybrid nanostructures for electrochemical energy storage. Nanoscale Horiz. 2016;1:27–40. doi:10.1039/C5NH00023H.
19. Xu D, Xuan C, Li X, Luo Z, Wang Z, Tang T, et al. Novel helical carbon nanotubes-embedded reduced graphene oxide in three-dimensional architecture for high-performance flexible supercapacitors. Electrochim Acta. 2020;339:135912. doi:10.1016/j.electacta.2020.135912.
20. Liang J, Xiang C, Zou Y, Hu X, Chu H, Qiu S, et al. Spacing graphene and Ni-Co layered double hydroxides with polypyrrole for high-performance supercapacitors. J Mater Sci Technol. 2020;55:190-7. doi:10.1016/j.jmst.2019.10.030.
21. Qi J, Chen Y, Li Q, Sui Y, He Y, Meng Q, et al. Hierarchical NiCo layered double hydroxide on reduced graphene oxide-coated commercial conductive textile for flexible high-performance asymmetric supercapacitors. J Power Sources. 2020;445:227342. doi:10.1016/j.jpowsour.2019.227342.
22. Liang YY, Bao SJ, Li HL. Nanocrystalline nickel cobalt hydroxides/ultrastable Y zeolite composite for electrochemical capacitors. J Solid State Electrochem. 2007;11:571-6. doi:10.1007/s10008-006-0197-9.
23. Song QS, Chiu CH, Chan SLI. Ball-milling processing of nanocrystalline nickel hydroxide and its effects in pasted nickel electrodes for rechargeable nickel batteries. J Solid State Electrochem. 2008;12:133-41. doi:10.1007/s10008-007-0370-9.
24. Ganesh V, Pitchumani S, Lakshminarayanan V. New symmetric and asymmetric supercapacitors based on high surface area porous nickel and activated carbon. J Power Sources. 2006;158:1523-32. doi:10.1016/j.jpowsour.2005.10.090.
25. Fang B, Gu A, Wang G, Li B, Zhang C, Fang Y, et al. Synthesis hexagonal β-Ni(OH)2 nanosheets for use in electrochemistry sensors. Microchim Acta. 2009;167:47–52. doi:10.1007/s00604-009-0213-8.
26. McKeown DA, Hagans PL, Carette LPL, Russell AE, Swider KE, Rolison DR. Structure of hydrous ruthenium oxides: implications for charge storage. J Phys Chem B. 1999;103:4825-32. doi:10.1021/jp990096n.
27. Liu R, Lee SB. MnO2/poly(3,4-ethylenedioxythiophene) coaxial nanowires by one-step coelectrodeposition for electrochemical energy storage. J Am Chem Soc. 2008;130:2942-3. doi:10.1021/ja7112382.
28. Subramanian V, Zhu H, Vajtai R, Ajayan PM, Wei B. Hydrothermal synthesis and pseudocapacitance properties of MnO2 nanostructures. J Phys Chem B. 2005;109:20207-14. doi:10.1021/jp0543330.
29. Wei J, Nagarajan N, Zhitomirsky I. Manganese oxide films for electrochemical supercapacitors. J Mater Process Technol. 2007;186:356-61. doi:10.1016/j.jmatprotec.2007.01.003.
30. Kulkarni SB, Jamadade VS, Dhawale DS, Lokhande CD. Synthesis and characterization of β-Ni(OH)2 up grown nanoflakes by SILAR method. Appl Surf Sci. 2009;255:8390-4. doi:10.1016/j.apsusc.2009.05.095.
31. Zhang S, Zeng HC. Self-assembled hollow spheres of β-Ni(OH)2 and their derived nanomaterials. Chem Mater. 2009;21:871-83. doi:10.1021/cm8028593.
32. Fu GR, Hu ZA, Xie LJ, Jin XQ, Xie YL, Wang YX, et al. Electrodeposition of nickel hydroxide films on nickel foil and its electrochemical performances for supercapacitor. Int J Electrochem Sci. 2009;4:1052-62. doi:10.1016/S1452-3981(23)15205-9.
33. Shao G, Yao Y, Zhang S, He P. Supercapacitor characteristic of La-doped Ni(OH)2 prepared by electrodeposition. Rare Met. 2009;28:132-6. doi:10.1007/s12598-009-0026-2.
34. Al-Osta A, Samer BS, Jadhav VV, Nakate UT, Mane RS, Naushad M. NiO@CuO@Cu bilayered electrode: two-step electrochemical synthesis supercapacitor properties. J Solid State Electrochem. 2017;21:2609-14. doi:10.1007/s10008-016-3489-8.

35. Xiao H, Yao S, Liu H, Qu F, Zhang X, Wu X. NiO nanosheet assembles for supercapacitor electrode materials. Prog Nat Sci Mater Int. 2016;26:271-5. doi:10.1016/j.pnsc.2016.05.007.
36. Tan Y, Liu Y, Kong L, Kang L, Ran F. Supercapacitor electrode of nano-Co3O4 decorated with gold nanoparticles via in-situ reduction method. J Power Sources. 2017;363:1–8. doi:10.1016/j.jpowsour.2017.07.054.
37. Gupta V, Kusahara T, Toyama H, Gupta S, Miura N. Potentiostatically deposited nanostructured α-Co(OH)2: a high performance electrode material for redox-capacitors. Electrochem Commun. 2007;9:2315-9. doi:10.1016/j.elecom.2007.06.041.
38. Lu X, Zeng Y, Yu M, Zhai T, Liang C, Xie S, et al. Oxygen-deficient hematite nanorods as high-performance and novel negative electrodes for flexible asymmetric supercapacitors. Adv Mater. 2014;26:3148-55. doi:10.1002/adma.201305851.
39. Wang D, Li Y, Wang Q, Wang T. Nanostructured Fe2O3-graphene composite as a novel electrode material for supercapacitors. J Solid State Electrochem. 2012;16:2095-102. doi:10.1007/s10008-011-1620-4.
40. Lee KK, Deng S, Fan HM, Mhaisalkar S, Tan HR, Tok ES, et al. α-Fe2O3 nanotubes-reduced graphene oxide composites as synergistic electrochemical capacitor materials. Nanoscale. 2012;4:2958-61. doi:10.1039/c2nr11902a.
41. Bhise SC, Awale DV, Vadiyar MM, Patil SK, Kokare BN, Kolekar SS. Facile synthesis of CuO nanosheets as electrode for supercapacitor with long cyclic stability in novel methyl imidazole-based ionic liquid electrolyte. J Solid State Electrochem. 2017;21:2585-91. doi:10.1007/s10008-016-3490-2.
42. Su X, Feng G, Yu L, Li Q, Zhang H, Song W, et al. In-situ green synthesis of CuO on 3D submicronporous/solid copper current collectors as excellent supercapacitor electrode material. J Mater Sci Mater Electron. 2019;30:3545-51. doi:10.1007/s10854-018-00632-y.
43. He D, Wang G, Liu G, Suo H, Zhao C. Construction of leaf-like CuO-Cu2O nanocomposites on copper foam for high-performance supercapacitors. Dalton Trans. 2017;46:3318-24. doi:10.1039/C7DT00287D.
44. Li Y, Wang X, Yang Q, Javed MS, Liu Q, Xu W, et al. Ultra-fine CuO nanoparticles embedded in three-dimensional graphene network nano-structure for high-performance flexible supercapacitors. Electrochim Acta. 2017;234:63–70. doi:10.1016/j.electacta.2017.02.167.
45. Li S, Gao A, Yi F, Shu D, Cheng H, Zhou X, et al. Preparation of carbon dots decorated graphene/polyaniline composites by supramolecular in-situ self-assembly for high-performance supercapacitors. Electrochim Acta. 2019;297:1094–1103. doi:10.1016/j.electacta.2018.12.036.
46. Yasoda KY, Mikhaylov AA, Medvedev AG, Kumar MS, Lev O, Prikhodchenko PV, et al. Brush like polyaniline on vanadium oxide decorated reduced graphene oxide: efficient electrode materials for supercapacitor. J Energy Storage. 2019;22:188-93. doi:10.1016/j.est.2019.02.010.
47. Zhuzhelskii DV, Tolstopjatova EG, Eliseeva SN, Ivanov AV, Miao S, Kondratiev VV. Electrochemical properties of PEDOT/WO3 composite films for high performance supercapacitor application. Electrochim Acta. 2019;299:182-90. doi:10.1016/j.electacta.2019.01.007.
48. Ravit R, Abdullah J, Ahmad I, Sulaiman Y. Electrochemical performance of poly(3,4-ethylenedioxythiophene)/nanocrystalline cellulose (PEDOT/NCC) film for supercapacitor. Carbohydr Polym. 2019;203:128-38. doi:10.1016/j.carbpol.2018.09.043.

